

Exploring the Conformational Dynamics of the Bovine ADP/ATP Carrier in Mitochondria

Martial Rey,^{†,‡,§,@} Eric Forest,^{*,‡,||,⊥} and Ludovic Pelosi^{*,†,‡,§}

[†]Commissariat à l'Energie Atomique et aux Energies Alternatives (CEA), Direction des Sciences du Vivant (DSV), Institut de Recherches en Technologies et Sciences pour le Vivant (iRTSV), Laboratoire de Biologie à Grande Echelle (BGE), Grenoble F-38054, France

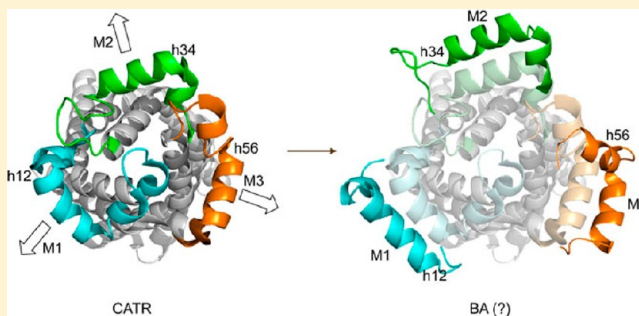
[‡]Université Joseph Fourier, Grenoble F-38000, France

[§]INSERM, U1038, Grenoble F-38054, France

^{||}CEA, DSV, Institut de Biologie Structurale, Grenoble F-38054, France

[⊥]UMR 5075 CNRS, Grenoble F-38027, France

ABSTRACT: The mitochondrial ADP/ATP carrier catalyzes the transport of ADP and ATP across the mitochondrial inner membrane by switching between two different conformations. They can be blocked by two inhibitors: carboxyatractyloside (CATR) and bongkreikic acid (BA). Our understanding of the ADP/ATP transport process is largely based on analysis of structural differences between the individual inhibited states. The X-ray crystallographic three-dimensional structure of bovine ADP/ATP carrier isoform 1 (bAnc1p) complexed with CATR was determined, but the structure of the BA-carrier complex remains unknown. We recently investigated the conformational dynamics of bAnc1p in detergent solution using hydrogen/deuterium exchange and mass spectrometry (HDX-MS). This study shed light on some features of ADP/ATP translocation, but the mechanism itself and the organization of bAnc1p in the membrane required further investigation. This paper describes the first study of bAnc1p in the mitochondria on the whole-protein scale using HDX-MS. Membrane-embedded bAnc1p was deuterated and purified under HDX-MS-compatible conditions. Our results for the carrier in the mitochondrial inner membrane differed from those published for the carrier in a detergent solution. These differences were mainly in the upper half of the cavity that globally showed a limited H/D exchange whatever the complex analyzed and at the level of the matrix loops that were less accessible to the solvent in the BA-carrier complex than in the CATR-carrier complex. They are discussed with respect to published data for bAnc1p and have provided new insights into the conformation of the matrix loops of the bovine carrier in complex with BA in mitochondria.



The adenine nucleotide carrier (Ancp) is located in the inner mitochondrial membrane where it catalyzes the transmembrane exchange of ADP and ATP between the intermembrane space (IMS) and the matrix compartments. ADP/ATP transport requires interconversion of Ancp between two conformational states that can be fixed by the specific transport inhibitors carboxyatractyloside (CATR) and bongkreikic acid (BA). These fixed conformations are termed CATR and BA, respectively, and are the basis of the single-binding site reorientation mechanism of the Ancp.^{1–3}

Ancp is the prime example of the mitochondrial carrier family (MCF). The atomic structure of bovine Anc1p (bAnc1p) trapped by CATR was determined at high resolution by our group.⁴ In this structure, the six transmembrane helices of bAnc1p (H1–H6) form a cavity with a deep cone-shaped depression, accessible only from the IMS. The odd-numbered helices are sharply kinked because of the presence of prolyl residues. These residues are involved in nucleotide binding and transport and in Ancp biogenesis⁵ and are part of the signature

sequences of the MCF members, PX(D/E)XX(K/R). Helices are connected to each other by IMS loops C1 and C2 and by matrix loops M1–M3 which include short α -helical stretches h12, h34, and h56, respectively. These helices align parallel to the surface of the membrane, where they strengthen the closed conformation of the CATR-carrier complex on the matrix side.⁴ In contrast to CATR-bound bAnc1p, the atomic structure of the bovine BA-inhibited form still remains unknown. However, bAnc1p complexed with CATR or BA has been characterized on the basis of how reactive various well-defined regions of the protein are to chemical, enzymatic, and immunochemical reagents. For example, bAnc1p was tested for accessibility to Lys- and Arg-specific proteases.^{6,7} Only the matrix loops of the BA-carrier complex were cleaved in inverted submitochondrial

Received: June 7, 2012

Revised: November 6, 2012

Published: November 8, 2012



particles. *N*-Ethylmaleimide, a SH-reactive reagent, was shown to target Cys56 (loop M1) in mitochondria only in the presence of BA, whereas CATR prevented labeling.⁸ Finally, the accessibility of the N-terminal extremity, which faces the IMS, to immunochemical labeling depends on the conformational state of bAnc1p in mitochondria.⁶ These combined results are consistent with a conformational transition on both sides of bAnc1p during ADP/ATP transport that is mimicked by the inhibitor-carrier complexes. This is also proposed for the yeast carrier via similar experimental approaches.^{9–14}

Recently, the solvent accessibility of bAnc1p conformations fixed by either CATR or BA was studied in a detergent solution by hydrogen/deuterium exchange and mass spectrometry (HDX-MS).¹⁵ This analysis provided new information about the detergent-extracted BA conformation and, thus, about the conformational dynamics of bAnc1p during ADP/ATP transport. Indeed, it was demonstrated that, on the matrix side, the BA-bAnc1p complex exhibits greater solvent accessibility than the CATR-bAnc1p complex. The reverse is true on the IMS side, suggesting that the cavity is closed on the IMS side and open toward the matrix in the detergent-extracted bAnc1p-BA complex.¹⁵ Similar results were obtained with the yeast carrier in another study combining HDX-MS, genetic, and biochemical approaches.¹⁶

However, in the case of the membrane-bound proteins, structural data in a detergent solution can be significantly different from data obtained *in organello* using biochemical approaches, making comparison difficult. Recent debates surrounding the biological validity of the atomic structure of the mitochondrial porin provide examples of how difficult this can be.^{17–19} Thus, although assessing the solvent accessibility of bovine Anc1p in a detergent solution provided new insights into the ADP/ATP translocation process,¹⁵ we must now go further if we are to determine the precise nucleotide exchange mechanism in use in mitochondria.

To achieve this aim, we have used HDX-MS to study the functional dynamics of bAnc1p in the mitochondria by analyzing CATR- and BA-carrier complexes. The carrier was deuterated in mitochondria, and then HDX-MS-compatible purification conditions were determined. Thus, we were able to study bAnc1p in its membrane environment. This is the first study to achieve such a feat. Our results are not entirely consistent with our previous work, in which bAnc1p was studied in a detergent solution. This suggests significant conformational changes, some of which probably occur during the detergent extraction step. These results are discussed with respect to the structural, conformational, and biochemical data available for bAnc1p in a detergent solution and mitochondria.

■ EXPERIMENTAL PROCEDURES

Chemicals. BA was prepared as previously described.²⁰ Hydroxylapatite (HTP) was from Bio-Rad. The polyclonal antibodies used in this work were generated in rabbits against SDS-treated bAnc1p. CATR was prepared in our laboratory. Commercial pepsin, bovine serum albumin (BSA), and trifluoroacetic acid were obtained from Sigma/Aldrich. Acetonitrile and dichloromethane were purchased from Carlo Erba Reagenti and Riedel de Haën, respectively.

Sodium Dodecyl Sulfate-Polyacrylamide Gel Electrophoresis (SDS-PAGE) and Western Blotting. Protein concentrations were determined using a BCA protein assay kit (Sigma/Aldrich) with BSA as a standard. For SDS-PAGE, samples were prepared as previously described.¹¹ Antibodies

directed against SDS-treated bAnc1p were used at a 1:2000 final dilution. Antibody binding was revealed using horseradish peroxidase (HRP)-coupled protein A and the enhanced chemiluminescence (ECL) system (Amersham Biosciences).

[³H]ATR Binding Assays. [³H]ATR binding assays of isolated mitochondria were performed as previously described.²¹ Briefly, bovine mitochondria were diluted (0.5–1 mg of protein/mL) in 1 mL of standard medium [0.12 M KCl, 10 mM Mops (pH 6.8), and 1 mM EDTA]. [³H]ATR was added at concentrations of up to 3.3 μ M. After incubation for 45 min at 4 °C, mitochondria were sedimented, and radioactivity associated with the pellet was determined by scintillation counting (Ready Value, Beckman). Assays were also performed in the presence of 20 μ M CATR to correct for minor nonspecific [³H]ATR binding in mitochondria.

Deuteration of Bovine Heart Mitochondria. The following steps were performed at 39 °C. Mitochondria (60 mg/mL of total protein) were exposed to CATR or BA (final concentration of 20 μ M) for 10 min. Then, HDX was initiated by 10-fold dilution in deuterated buffer containing 10 mM MOPS, 10 mM NaCl, and 1 mM EDTA (pH 6.8). The time course for the H/D exchange was followed over a 10000 s period by sequentially withdrawing 2 mg samples. These aliquots were immediately added to 20 μ L of quenching buffer containing 1 M glycine-HCl (pH 2.5), rapidly mixed, and flash-frozen in liquid nitrogen. Samples were stored in liquid nitrogen until they were analyzed.

Detergent Extraction of bAnc1p and Purification. The following steps were performed at 4 °C. Deuterated mitochondrial membranes were thawed in extraction buffer containing 200 mM glycine-HCl, 50 mM NaCl, 1 mM EDTA, and 1% (v/v) Triton X-100 (pH 2.5). The final protein concentration was 10 mg/mL. The suspension was placed on a HTP column prepared in a 1 mL syringe. The column had previously been equilibrated in buffer containing 10 mM MOPS, 10 mM NaCl, and 1 mM EDTA (pH 6.8) and then dried by centrifugation (3–4 mg of mitochondrial protein/mL of dry HTP). Deuterated bAnc1p was eluted under pressure using a piston. A purified bAnc1p solution was immediately diluted in 25 μ L of acidic buffer containing 100 mM glycine-HCl (pH 2.5).

Pepsin Proteolysis. bAnc1p was digested with pepsin as previously described.²² Briefly, 2 nmol of bAnc1p was digested in the presence of 1 M guanidinium chloride on a 1 mm \times 100 mm column packed with pepsin immobilized on POROS-20AL beads. The column was cooled in an ice bath at 0 °C during digestion.

High-Pressure Liquid Chromatography Peptide Separation. Peptides obtained by online protein digestion were loaded onto a peptide MicroTrap column (Michrom Bioresources, Auburn, CA). Samples were desalted by being washed with solution A [0.03% (v/v) TFA in water]; detergent is washed away with dichloromethane; this also removed the lipids.²² After re-equilibration of the trap column, gradient elution was started. Peptides were separated on a C18 reversed phase column (1 mm \times 100 mm, Jupiter, Phenomenex) using a linear gradient from 15 to 40% (v/v) solution B [95% (v/v) CH₃CN with 0.03% (v/v) TFA in water]. The gradient was applied over 20 min for deuterated samples or 40 min for peptide mapping experiments; 40% (v/v) solution B was then applied for 5 min at a flow rate of 50 μ L/min. The remainder of the gradient was made up with solution A. Before peptide separation, the column was equilibrated with 15% (v/v) B. To minimize back-exchange,

the valves, trap column, and analytical column were cooled to 0 °C by being immersed in an ice–water bath.

MS Analyses. Deuterated samples were analyzed, and accurate mass measurements were taken on a liquid chromatography electrospray time-of-flight MS (LC ESI-ToF-MS) 6210 system (Agilent Technologies). Isotope envelopes were extracted using Mass Hunter Qualitative Analyses (Agilent Technologies). The centroid of the isotopic distribution was measured with MagTran.²³ Carrier mapping was represented using DrawMap, available at <http://ms.biomed.cas.cz/MSTools/>.

RESULTS

bAnc1p Content in Mitochondria. The bAnc1p content of mitochondria was determined through [³H]ATR binding experiments. ATR is a specific Ancp inhibitor. For our calculations, we assumed that 1 mol of ATR binds to 1 mol of transport unit. The maximal number of binding sites obtained was 1080 ± 65 pmol/mg of total protein, which is in line with numerical data in the literature.²⁴

Optimizing Deuteration of Bovine Heart Mitochondria. We first assessed the optimal temperature for bAnc1p labeling, based on labeling of the CATR–carrier complex in mitochondrial membranes. Bovine heart mitochondria were incubated for 2 h in a deuterated buffer as described in Experimental Procedures. Under these conditions, we suppose that mitochondria are fully equilibrated in deuterium. Different temperatures ranging from 4 to 39 °C were tested. Deuterated bAnc1p complexed to CATR was then extracted and purified as described below. Deuterium labeling was analyzed by MS as previously described.²² The level of deuterium incorporated was calculated for six peptides identified previously.¹⁵ The results are shown in Figure 1A. Deuteration of these peptides was improved at temperatures of ≥ 21 °C. This result is likely related to the melting temperature of the mitochondrial membranes, which is ~ 17 °C. Similar data were obtained with bAnc1p trapped by BA (data not shown). On the basis of this result, all subsequent deuterium labeling experiments were performed at 39 °C, which corresponds to the *in vivo* temperature of the bovine heart.

Detergent Extraction of Deuterated bAnc1p under HDX-MS-Compatible Conditions. Deuterated bAnc1p complexed with either CATR or BA (1 mg of total protein) was extracted from mitochondrial membranes using HDX-MS analysis-compatible detergents and conditions (where H/D back-exchange is minimized), i.e., pH 2.5 (glycine buffer), at 4 °C in the presence of Triton X-100, which is suitable for HDX-MS studies.^{15,16,22} The effect of various incubation times in the detergent solution, ranging from a few seconds to 30 min, was tested. Suspensions were centrifuged at 10000g for 10 min. The supernatants, corresponding to the Triton X-100-extracted proteins, were analyzed by Western blotting using antibodies raised against SDS-treated bAnc1p. As shown in Figure 1B, Triton X-100 was capable of instantly solubilizing bAnc1p at maximal levels under HDX-compatible conditions (Figure 1B, lane 1). Similar results were obtained with bAnc1p complexed to BA (results not shown). This condition was used in the remainder of the study.

HTP Purification of Triton X-100-Extracted Deuterated bAnc1p and Assessment of H/D Back-Exchange during Purification. bAnc1p is generally purified by gravity-flow on a HTP column.²⁵ This is of interest as it purifies the bovine carrier in a single step. However, the calcium phosphate crystals forming the HTP powder are soluble in acid. Under this condition, the

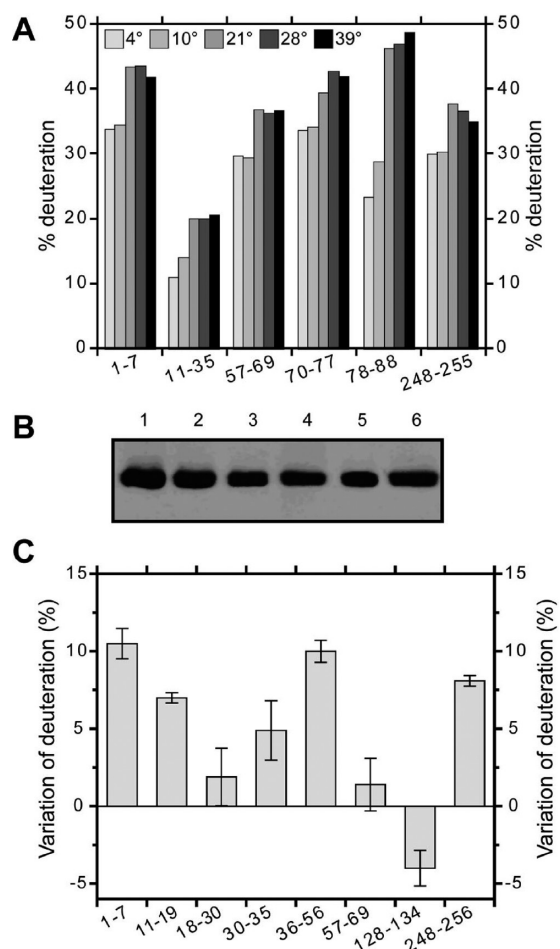


Figure 1. HDX-MS-compatible preparation of bAnc1p complexed to either CATR or BA after mitochondrial deuteration. (A) bAnc1p as a CATR–carrier complex was labeled with deuterium *in situ* in the mitochondrial membranes at temperatures ranging from 4 to 39 °C over 2 h. After HTP purification, the level of deuterium incorporation was calculated for six peptides located at different positions along the protein sequence. (B) bAnc1p in complex with CATR was extracted from mitochondria using Triton X-100 (see Experimental Procedures). Several incubation times were tested: instantly (lane 1), 30 s (lane 2), 1 min (lane 3), 5 min (lane 4), 10 min (lane 5), and 30 min (lane 6). Ten microliters of Triton X-100-extracted protein was loaded in each lane. Solubilized proteins were analyzed by Western blotting using antibodies raised against SDS-treated bAnc1p. Immune complexes were revealed by protein-A–HRP ECL. (C) Assessing H/D back-exchange during purification of the deuterated CATR–bAnc1p complex. Purified bAnc1p trapped by CATR was deuterated in a detergent solution, as previously described in ref 15, and then passed through the HTP column (experiment performed in triplicate). Variation of deuteration was calculated for eight peptides located throughout the protein sequence.

pH of the carrier preparation increases to approximately 7, which may lead to a significant back-exchange of the deuterium. The HTP purification method was nevertheless selected but was modified to shorten the time necessary for elution of the carrier from the column (see Experimental Procedures). This minimized back-exchange. Lysate was prepared at a concentration of 10 mg/mL. Different column:lysate volume ratios were tested. This revealed the optimal ratio to be 3 (results not shown). The sample volume and the amount of pure protein to be analyzed in MS were also adjusted. The best results were obtained with 200 μ L of deuterated mitochondrial lysates

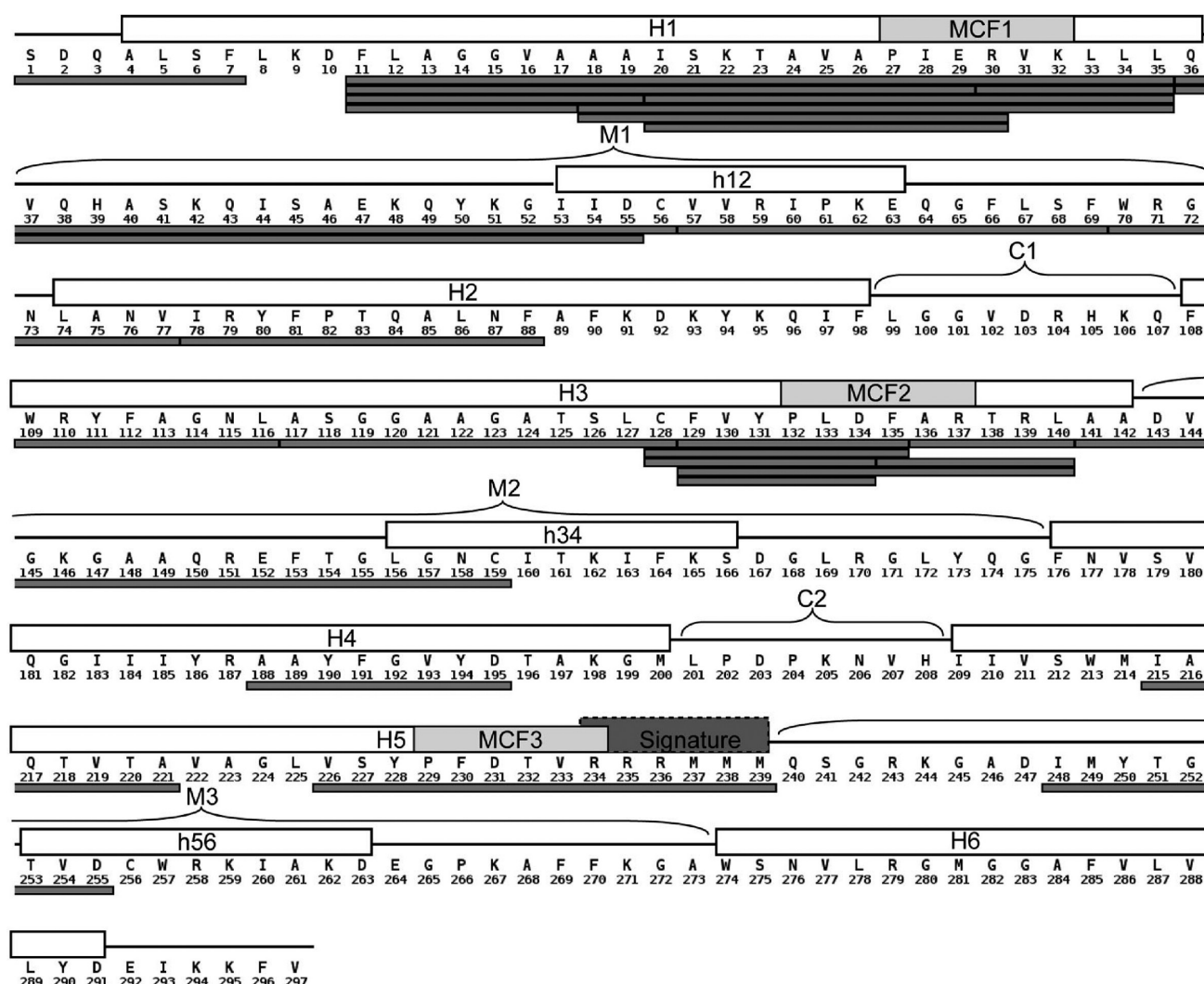


Figure 2. Peptide mapping of bAnc1p used in HDX-MS experiments after immobilized pepsin digestion. All the peptides identified by ESI-Trap-MS/MS analyses are represented under the primary amino acid sequence by gray bars. Transmembrane helices (H1–H6), matrix loops (M1–M3), encompassing matrix helices (h12, h34, and h56), and IMS loops (C1 and C2), as determined in the bAnc1p three-dimensional structure, are shown above the sequence. The MCF motifs, i.e., PX(D/E)XX(K/R), and the Ance signature sequence (RRRMMM) are indicated above the sequence by the light gray and dark gray rectangles, respectively.

containing ~2 nmol of bAnc1p for each measurement of HDX kinetics analysis.

To minimize back-exchange after elution of deuterated bAnc1p complexed to CATR from the HTP column, it was immediately diluted in acidic buffer. Deuteration levels were measured for several characteristic bAnc1p peptides before and after they had passed through the HTP column to assess back-exchange. bAnc1p complexed to CATR was purified and then deuterated in the presence of Triton X-100, as previously described.¹⁵ The purified–deuterated complex frozen at pH 2.5 was filtered through the HTP column. The purification method induced an overall loss of deuteration for all peptides analyzed, from approximately 2% (peptide 57–69) to 10% (peptides 1–7 and 36–56) (Figure 1C). These differences are limited and should not affect our interpretations. Consequently, it is possible to purify bAnc1p on a column of HTP in a single step with acceptable levels of back-exchange. A similar range of loss of deuteration was observed for peptides from the BA–carrier complex (data not shown). The positive deuteration change obtained for peptide 128–134 is probably caused by its low

intensity and should be considered as an artifact as we reached the sensibility limit of the spectrometer under our HDX conditions.

bAnc1p Peptide Mapping. bAnc1p as a CATR– or BA–carrier complex was digested with pepsin as described previously,²⁶ i.e., by online proteolysis using a column packed with immobilized pepsin. HDX-MS analysis resulted in 58% protein coverage [29 peptides (Figure 2)]. This was slightly lower than the coverage obtained in a detergent solution (72% and 37 peptides).¹⁵ As in our previous work,¹⁵ the N-terminal half of bAnc1p was much better covered than the C-terminal region, with 85% coverage for region 1–159 (25 peptides). Some of these peptides overlapped, thus increasing the spatial resolution for peptide regions 11–35 and 128–140, which encompass the first and second MCF motifs, respectively (Figure 2). Sequence coverage for the other part of the carrier (from residue 160 to 297) was lower (27%), with only four peptides. The pepsin digestion pattern also provided several pairs of overlapping peptides differing by only one residue (Figure 2). Two of these, residues 50–55 and 50–56, provided precise HDX

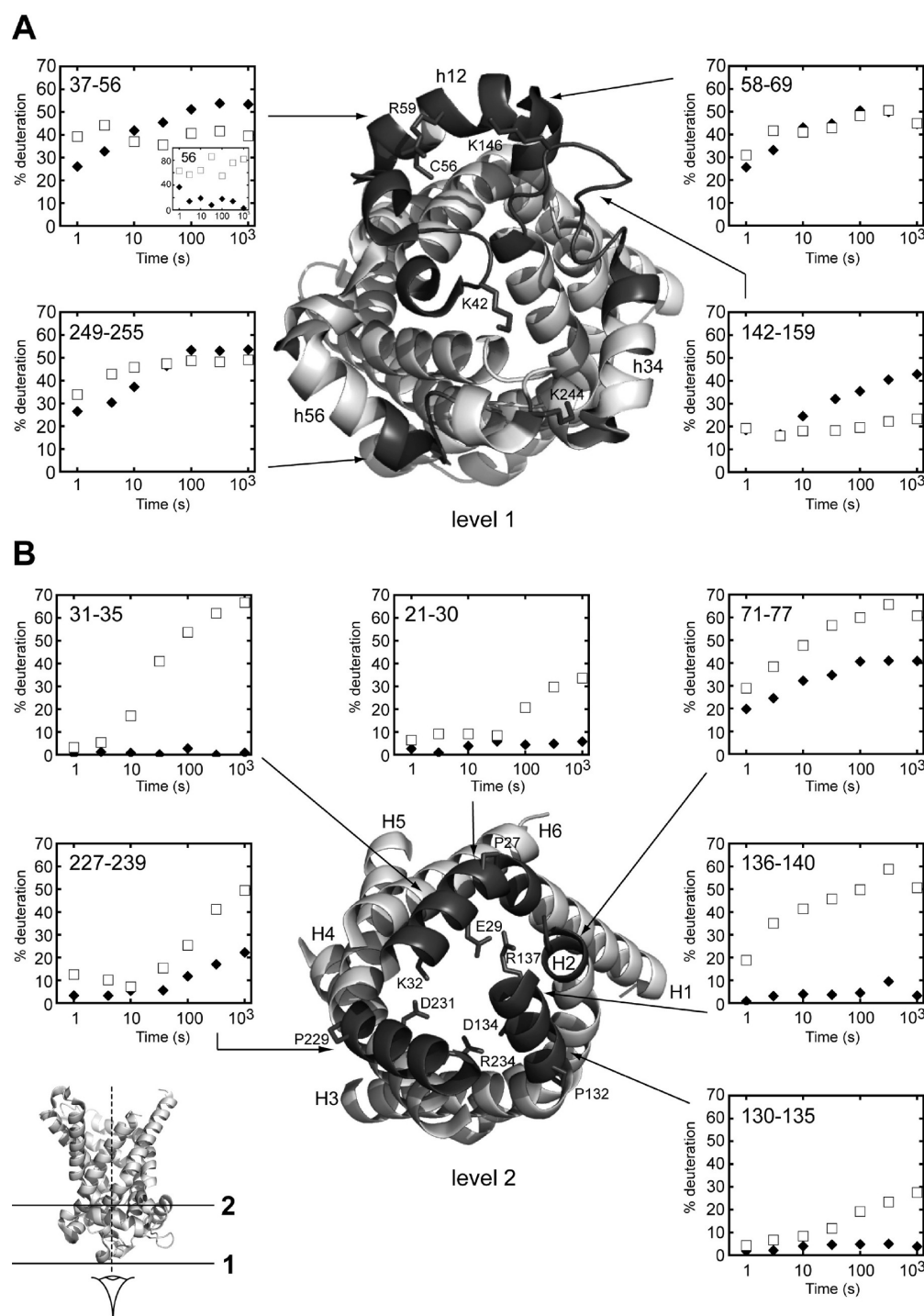


Figure 3. HDX kinetics for bAnc1p on the matrix side mapped on the crystal structure of bAnc1p in complex with CATR. The dark gray ribbons represent the regions covered by the peptides analyzed. Transmembrane α -helices H1–H6 and matrix helices h12, h34, and h56 are labeled. (A) Structure from the matrix side (level 1). Residues Lys42, Arg59, Lys146, and Lys244 that are targeted by Lys/Arg-specific proteases only in the BA-carrier complex. Residue Cys56 is labeled by the SH reagent only in the presence of BA. The inset shows HDX kinetics for amide proton 56 (Cys56), deduced from pairs of overlapping peptides (36–55 and 36–56). (B) Structure shown at level 2 and seen from below. Residues involved in the MCF signature motifs (Pro27, Glu29, Lys32, Pro132, Asp134, and Arg137) are labeled. Units of time for the HDX kinetics are given in seconds. HDX is expressed as a percentage relative to maximal theoretical level of deuteration. HDX kinetics for regions specific to the CATR-carrier complex and the BA-carrier complex are shown with filled diamonds and empty squares, respectively.

information for Cys56. This residue was also biochemically characterized in the bovine mitochondrial inner membrane using an SH-reactive reagent.⁸

Position of Matrix Loops Relative to the Membrane in bAnc1p Complexed with either CATR or BA. In the three-

dimensional structure,⁴ loops M1–M3 are positioned parallel to the surface of the membrane, where they appear to strengthen the closed conformation of the bovine carrier on the matrix side when complexed to CATR. These loops include short α -helical stretches h12, h34, and h56, respectively. In our study, loop M1

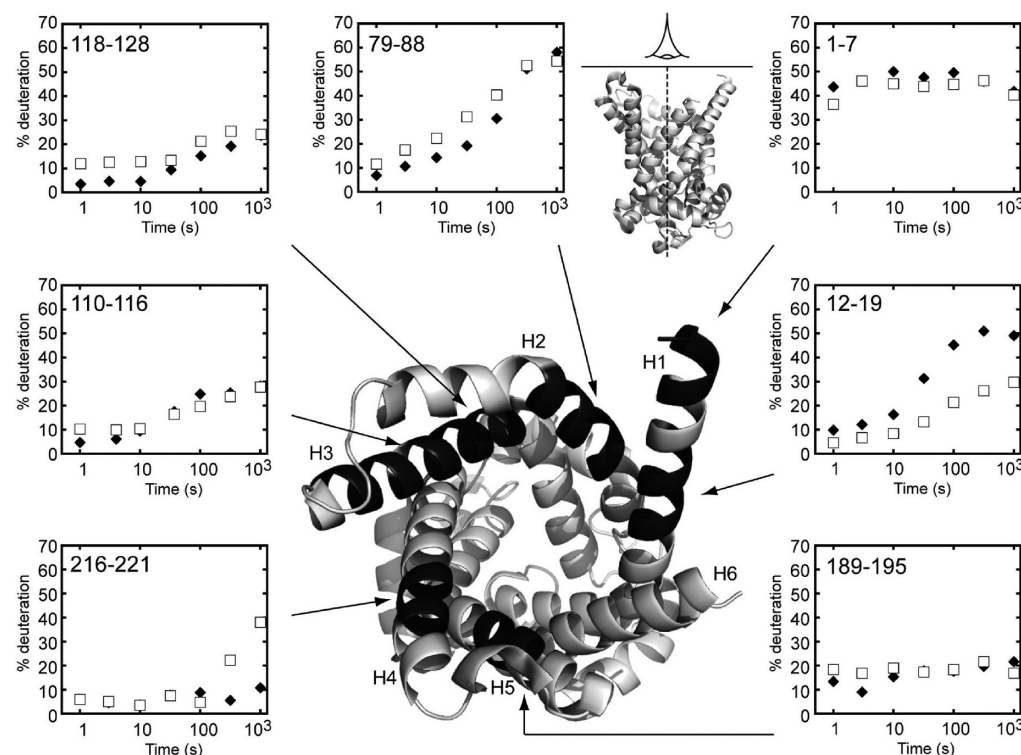


Figure 4. HDX kinetics for bAnc1p on the intermembrane side mapped on the crystal structure of bAnc1p complexed to CATR. The dark gray ribbons represent the regions covered by the peptides analyzed. Transmembrane α -helices H1–H6 are labeled. For further description, see the legend of Figure 3.

was partly covered by peptides in regions 37–56 and 58–69, loop M2 by region 142–159, and loop M3 by region 249–255 (Figure 3A). In the CATR–carrier complex, the HDX kinetics for all these regions were similar. However, the amide protons of regions 37–56, 58–69, and 249–256 generally exchanged more rapidly than those of region 142–159. A significantly higher level of deuteration was also observed at the end of the experiment (53, 50, and 54% vs 43% of HDX, respectively). Except for region 149–159, the extent of deuteration was quite high after HDX for only 10 s (close to 40% exchange). This is in line with the positions of all these regions, which are exposed to the solvent (Figure 3A), but region 149–159 is slightly less exposed to deuterium than the other three.

The results obtained with the BA–carrier complex were more surprising. Overall, regions 58–69 and 249–255 presented HDX kinetics similar to those for the CATR–carrier complex (Figure 3A). In contrast, region 142–159 was protected from deuteration in the presence of BA (23% of HDX at the end of the experiment), and region 37–56 was deuterated faster in the presence of BA than in the presence of CATR. However, the CATR–carrier complex was still more extensively deuterated at the end of the experiment (53% of HDX in the presence of CATR vs 39% of HDX in the presence of BA) (Figure 3A). These results did not occur with our previously published data for HDX of bAnc1p in a detergent solution.¹⁵ This discrepancy is discussed below.

Pepsin digestion produced a pair of overlapping peptides (36–55 and 36–56) differing by only one residue, Cys56. As shown in our previous study, inhibitor-related Cys56 deuteration could be assessed by a subtractive approach.¹⁵ Analysis of the Cys56 amide showed a higher rate of deuterium uptake in the presence of BA than in the presence of CATR (Figure 3A, inset). This is in agreement with data from biochemical studies, where the SH

group of Cys56 was better labeled by SH-reactive reagents in the BA–carrier complex than in the CATR–carrier complex.⁸

Conformationally Related Accessibility of the Carrier Cavity Analyzed by Local HDX in the Presence of either CATR or BA. The lower part of the carrier cavity, toward the matrix, was mainly covered by peptides from regions 21–30 (helix H1), 31–35 (helix H1), 71–77 (helix H2), 130–135 (helix H3), 136–140 (helix H3), and 227–239 (helix H5). As presented in Figure 3B, the amide protons of all these regions were more rapidly and extensively exchangeable with deuterium when bAnc1p was complexed with BA rather than CATR (34, 67, 61, 27, 51, and 49% vs 6, 1, 41, 4, 3, and 22% of HDX, respectively, at the end of the experiment). These results are consistent with the bottom of the cavity being more exposed to solvent in the BA conformer than in the CATR conformer, as shown previously in a detergent solution.¹⁵

Helix H1 was covered by regions 1–7, 12–19, 21–30, and 31–35 (Figure 2). As shown in Figures 3A and 4, its N-terminal extremity (region 1–7) was extensively and rapidly deuterated in the presence of both inhibitors. The N-terminal half of helix H1 (region 12–19) underwent better deuterium exchange in the CATR–carrier complex (49% of HDX at the end of the experiment) than in the BA–carrier complex (30% of HDX), and the opposite was true for its C-terminal half, covered by regions 21–30 and 31–35. The reversal in deuterium exchange takes place at the level of the first MCF motif (Figure 2). These data thus suggest that the N-terminal part of helix H1 is more exposed to the solvent in the CATR conformer, as indicated in the three-dimensional structure. They also underline the pivotal role played by the first MCF motif in the conformational changes that occur in the carrier cavity upon inhibitor binding.

Except for regions 12–19 and 216–221, the remainder of the upper half of the cavity (regions 79–88, 110–116, 118–128, and

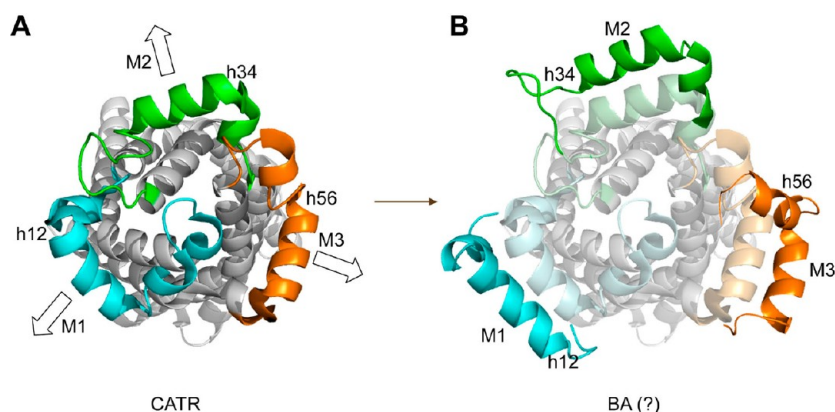


Figure 5. (A) Architecture of bAnc1p as ribbon diagrams viewed from the matrix side. (B) Hypothetical model of repositioning of loops M1–M3 from the bottom of the cavity to the matrix side of the inner membrane when BA binds. This would also lead to matrix helices rotating on themselves to make the side chains more accessible to chemical and enzymatic reagents. Corresponding matrix helices h12, h34, and h56 are labeled. The ribbon diagram was drawn using PyMOL version 0.99 (DeLano Scientific LLC).

189–195) presented similar deuterium exchange kinetics with both inhibitors (Figure 4). This behavior was observed throughout the time course of the experiment for regions 110–116 (helix H3), 118–128 (helix H3), and 189–195 (helix H4). Interestingly, the extent of deuterium exchange remains low (<30% of HDX at the end of the experiment). No difference in solvent accessibility was found for region 79–88 either, although this region was much more extensively deuterated at the end of the experiment (~54–58% of HDX). Region 216–221 (helix H5) also exchanged very slowly in both complexes for the first 100 s of HDX but, surprisingly, was more readily deuterated at the end of the experiment in the BA–carrier complex (38% of HDX) than in the CATR–carrier complex (11% of HDX). All these results differ from those obtained for the carrier in a detergent solution¹⁵ and are discussed below.

DISCUSSION

HDX-MS experiments provide information about the local structure and dynamics of proteins and have been successfully employed in our laboratory to provide new insights into the conformational dynamics of detergent-extracted bAnc1p complexed to either CATR or BA.¹⁵ The results obtained from HDX-MS experiments fully account for the three-dimensional structure of bAnc1p complexed to CATR. They also support a mechanism for translocation of ADP from the IMS to the matrix based on a single-site reorientation mechanism of Ancp as suggested in the past (see ref 27 for a review). The intrinsic flexibility of the odd-numbered helices, coupled to a conformational transition of the matrix loops, would lead to opening of the cavity toward the matrix, in the BA conformation.¹⁵ The cavity was suggested to close on the IMS to account for the limited incorporation of deuterium in this region of bAnc1p complexed to BA.¹⁵ This model was based on the analysis of the protein in a detergent solution. Its validation required further investigations *in situ* in mitochondria.

Data related to the bovine carrier in the mitochondrial membrane were published but remained limited to studies of well-defined regions of the protein and their reactivity with chemical, enzymatic, and immunochemical reagents.²⁸ To improve our knowledge of the precise mechanisms involved in nucleotide exchange in mitochondria with whole proteins, we developed a method for purifying deuterated bAnc1p complexed to either CATR or BA from mitochondria under conditions

involving minimal back-exchange and compatible with HDX-MS. This method allowed us to investigate the conformational dynamics of bAnc1p *in organello*. From HDX-MS data, we did not gain any evidence of multimeric structures of bAnc1p *in situ* in mitochondria (this work) or in a detergent solution.¹⁵ These results were consistent with a monomeric structure of Ancp as recently described in the literature.^{29–32} They were therefore discussed in the following assuming the complexes are monomeric.

The greatest differences in deuteration levels between complexes were observed for regions located at the bottom of the cavity. They were more extensively deuterated in the presence of BA than in the presence of CATR (Figure 3). Some of these regions encompass the MCF motifs and the Ancp signature sequence. This greater accessibility in complex with BA was similar to what was observed in a detergent solution with bAnc1p and with yeast isoform 2 Ancp.^{15,16} All these data are consistent with the lower part of the cavity being open toward the mitochondrial matrix when bAnc1p is complexed with BA. However, our study of bAnc1p *in situ* in the membrane revealed that in the BA–carrier complex, the matrix loops presented a solvent accessibility pattern different from that reported in a detergent solution. Indeed, in the membrane, they did not exhibit faster deuteration in the BA–carrier complex than in the CATR–carrier complex, in contrast with experiments with detergent-solubilized complexes.¹⁵ Their deuteration is similar (loops M1 and M3) with both inhibitors or is lower (loop M2) in the presence of BA than in the presence of CATR. We do not fully understand this difference. In the BA–carrier complex studied in a detergent solution, it is possible that the more rapid and extensive deuteration of the matrix loops might be due to a misfolded conformation because of the possible loss of BA. However, this hypothesis was not considered in our comparative study. Indeed, for peptides covering these regions, only one type of HDX kinetics was obtained,¹⁵ and the solvent accessibility of bAnc1p isolated without inhibitor was always different from that of the complexed form with either CATR or BA. Deuteration of the noninhibited carrier was much faster and stronger throughout the carrier sequence probably because of a nonstabilized conformation in the absence of inhibitor (M. Rey et al., unpublished data). We propose instead that our data might reflect repositioning of loops M1–M3 from the bottom of the cavity to the matrix side of the inner membrane when BA binds

(Figure 5). This repositioning would cause the cavity to open, while also partially masking the loops to the solvent. This structural change would be less marked or not possible in a Triton X-100 micelle, resulting in sliding of the matrix loops into the solvent and thus better deuterium exchange, as reported previously.¹⁵

The accessibility of the bAnc1p matrix loops to Lys- or Arg-specific proteases was previously investigated in the presence of inhibitors.^{6,7} Only the BA-carrier complex was cleaved in inside-out submitochondrial particles at Lys42, Arg59, Lys146, and Lys244, all of which are located in the matrix loops. In addition, in mitochondria, *N*-ethylmaleimide, an SH-reactive reagent, labeled Cys56 (loop M1) only in the presence of BA, whereas CATR prevented its labeling.⁸ In the study presented here, the single-residue Cys56 amide showed a higher rate of deuterium uptake in the presence of BA, thus corroborating the biochemical results.⁸ In the bovine CATR-carrier complex, the side chains of the residues targeted are stuck against the bottom of the cavity (Lys42, Arg59, and Lys146) or are oriented toward the inside of the cavity (Cys56 and Lys244), leading to their low level of exposure to the solvent. In the BA-carrier complex, they could be unmasked by repositioning of the matrix loops in the carrier structure, as hypothesized above. Additionally, as residues Cys56 and Arg59 are located in the α -helical stretch (h12), it is likely that the movement of loop M2 to a position close against the membrane (as proposed above) leads to h12 rotating on itself to make the side chains more accessible.

Most of the other regions located in the upper part of the cavity, toward the IMS, presented small differences in solvent accessibility. This is the case for regions 79–88 (helix H2), 118–128 (helix H3), and 189–195 (helix H4) throughout the time course of the labeling experiment, and for region 216–221 (helix H5) before 100 s of HDX. Except for region 79–88, all these regions remained weakly deuterated overall in both complexes. The low level of deuteration measured in this part of the cavity in the BA-carrier complex supports the hypothesis that it is closed on the IMS side as previously suggested.¹⁵ In contrast, the results obtained with the CATR-carrier complex were more difficult to interpret when the structure of the bovine carrier trapped by CATR is considered. Indeed, in our previous study, we have shown in a detergent solution that this complex was readily accessible to the solvent toward the IMS compared to the BA-carrier complex. This result was in agreement with an opening of the upper part of the cavity on the IMS side in the CATR conformation and its closing in the BA conformation being explained by the limited deuterium incorporation recorded.¹⁵ To explain this difference, we therefore propose that this part of the cavity in the CATR-carrier complex is more protected from deuteration *in situ* in mitochondria than it is in a detergent solution, suggesting it is partially buried in the lipid bilayer and/or a much tighter conformation of the peptide chain that could become relaxed during the extraction of detergent. It is also possible that protein partners, masking the upper part of the cavity in all conformations, are present in the mitochondrial inner membrane.

CONCLUSION

Our study highlights significant differences in the conformational dynamics of bAnc1p studied either in a detergent solution¹⁵ or embedded into the mitochondrial membrane (this work). Indeed, in the BA-carrier complex, matrix loops were globally slightly more protected from deuteration in mitochondria than in the CATR-carrier complex, and the upper part of the cavity in

the CATR-complex was also unexpectedly weakly deuterated overall as in the BA-carrier complex. However, the lower part of the cavity, which contains the MCF motifs, maintains a higher level of deuterium exchange in the BA-carrier complex than in the CATR-carrier complex, which is consistent with an opening of this part of the cavity toward the matrix in the BA-carrier complex. Our results support relocation of the matrix loops from the bottom of the cavity to the matrix side of the inner membrane. Rotation of matrix helices, such as h12, on themselves during the conformational transition is also hypothesized to explain how some residues become more accessible to the solvent in the matrix compartment. This model will be further investigated by molecular dynamics simulations.

AUTHOR INFORMATION

Corresponding Author

*L.P.: BGE, iRTSV, CEA de Grenoble, 17 avenue des Martyrs, 38054 Grenoble Cedex 9, France; phone, +33 (0)438783476; e-mail, ludovic.pelosi@cea.fr. E.F.: IBS, 41 rue Jules Horowitz, 38027 Grenoble cedex 1, France; phone, +33 (0)438783403; e-mail, eric.forest@ibs.fr.

Present Address

@Department of Biochemistry and Molecular Biology, Faculty of Medicine, University of Calgary, HSc. B031, 3330 Hospital Dr. NW, Calgary, Alberta T2N 4N1, Canada.

Funding

This work was supported by grants from the University Joseph Fourier, the Centre National de la Recherche Scientifique, and the Commissariat à l'Energie Atomique et aux Energies Alternatives (program Signalisation et Transport Membranaire). M.R. was supported by a fellowship from the Université Joseph Fourier.

Notes

The authors declare no competing financial interest.

ACKNOWLEDGMENTS

We thank Drs. Gérard Klein and Gérard Brandolin for constructive discussions and technical assistance.

ABBREVIATIONS

MCF, mitochondrial carrier family; CATR, carboxyatractyloside; BA, bongkreic acid; IMS, mitochondrial intermembrane space; Ancp, ADP/ATP carrier; bAnc1p, bovine isoform 1 Ancp; HDX, hydrogen/deuterium exchange; MS, mass spectrometry; ESI, electrospray ionization; HTP, hydroxylapatite; SDS, sodium dodecyl sulfate.

REFERENCES

- (1) Erdelt, H., Weidemann, M. J., Buchholz, M., and Klingenberg, M. (1972) Some principle effects of bongkreic acid on the binding of adenine nucleotides to mitochondrial membranes. *Eur. J. Biochem.* 30, 107–122.
- (2) Klingenberg, M., and Buchholz, M. (1973) On the mechanism of bongkreic acid effect on the mitochondrial adenine-nucleotide carrier as studied through the binding of ADP. *Eur. J. Biochem.* 38, 346–358.
- (3) Buchanan, B. B., Eiermann, W., Riccio, P., Aquila, H., and Klingenberg, M. (1976) Antibody evidence for different conformational states of ADP, ATP translocator protein isolated from mitochondria. *Proc. Natl. Acad. Sci. U.S.A.* 73, 2280–2284.
- (4) Pebay-Peyroula, E., Dahout-Gonzalez, C., Kahn, R., Trézéguet, V., Lauquin, G. J. M., and Brandolin, G. (2003) Structure of mitochondrial ADP/ATP carrier in complex with carboxyatractyloside. *Nature* 426, 39–44.

- (5) Babet, M., Blancard, C., Pelosi, L., Lauquin, G. J. M., and Trézéguet, V. (2012) The transmembrane prolines of the mitochondrial ADP/ATP carrier are involved in nucleotide binding and transport and in its biogenesis. *J. Biol. Chem.* 287, 10368–10378.
- (6) Brandolin, G., Boulay, F., Dalbon, P., and Vignais, P. V. (1989) Orientation of the N-terminal region of the membrane-bound ADP/ATP carrier protein explored by antipeptide antibodies and an arginine-specific endoprotease. Evidence that the accessibility of the N-terminal residues depends on the conformational state of the carrier. *Biochemistry* 28, 1093–1100.
- (7) Marty, I., Brandolin, G., Gagnon, J., Brasseur, R., and Vignais, P. V. (1992) Topography of the membrane-bound ADP/ATP carrier assessed by enzymatic proteolysis. *Biochemistry* 31, 4058–4065.
- (8) Boulay, F., and Vignais, P. V. (1984) Localization of the N-ethylmaleimide reactive cysteine in the beef heart mitochondrial ADP/ATP carrier protein. *Biochemistry* 23, 4807–4812.
- (9) Majima, E., Shinohara, Y., Yamaguchi, N., Hong, Y. M., and Terada, H. (1994) Importance of loops of mitochondrial ADP/ATP carrier for its transport activity deduced from reactivities of its cysteine residues with the sulfhydryl reagent eosin-5-maleimide. *Biochemistry* 33, 9530–9536.
- (10) Kihira, Y., Iwashita, A., Majima, E., Terada, H., and Shinohara, Y. (2004) Twisting of the second transmembrane α -helix of the mitochondrial ADP/ATP carrier during the transition between two carrier conformational states. *Biochemistry* 43, 15204–15209.
- (11) Dahout-Gonzalez, C., Ramus, C., Dassa, E. P., Dianoux, A. C., and Brandolin, G. (2005) Conformation-dependent swinging of the matrix loop m2 of the mitochondrial *Saccharomyces cerevisiae* ADP/ATP carrier. *Biochemistry* 44, 16310–16320.
- (12) Kihira, Y., Majima, E., Shinohara, Y., and Terada, H. (2005) Cysteine labeling studies detect conformational changes in region 106–132 of the mitochondrial ADP/ATP carrier of *Saccharomyces cerevisiae*. *Biochemistry* 44, 184–192.
- (13) Iwashita, A., Kihira, Y., Majima, E., Terada, H., Yamazaki, N., Kataoka, M., and Shinohara, Y. (2006) The structure of the second cytosolic loop of the yeast mitochondrial ADP/ATP carrier AAC2 is dependent on the conformational state. *Mitochondrion* 6, 245–251.
- (14) Kihira, Y., Ueno, M., and Terada, H. (2007) Difference between yeast and bovine mitochondrial ADP/ATP carriers in terms of conformational properties of the first matrix loop as deduced by use of copper-o-phenanthroline. *Biol. Pharm. Bull.* 30, 885–890.
- (15) Rey, M., Man, P., Cléménçon, B., Trézéguet, V., Brandolin, G., Forest, E., and Pelosi, L. (2010) Conformational dynamics of the bovine mitochondrial ADP/ATP carrier isoform 1 revealed by hydrogen/deuterium exchange coupled to mass spectrometry. *J. Biol. Chem.* 285, 34981–34990.
- (16) Cléménçon, B., Rey, M., Trézéguet, V., Forest, E., and Pelosi, L. (2011) Yeast ADP/ATP carrier isoform 2: conformational dynamics and role of the RRRMMM signature sequence methionines. *J. Biol. Chem.* 286, 36119–36131.
- (17) Colombini, M. (2009) The published 3D structure of the VDAC channel: Native or not? *Trends Biochem. Sci.* 34, 382–389.
- (18) Colombini, M. (2012) VDAC structure, selectivity, and dynamics. *Biochim. Biophys. Acta* 1816, 1457–1465.
- (19) Hiller, S., Abramson, J., Mannella, C., Wagner, G., and Zeth, K. (2010) The 3D structures of VDAC represent a native conformation. *Trends Biochem. Sci.* 35, 514–521.
- (20) Lauquin, G. J. M., and Vignais, P. V. (1976) Interaction of (³H)bongkreic acid with the mitochondrial adenine nucleotide translocator. *Biochemistry* 15, 2316–2322.
- (21) Brandolin, G., Meyer, C., Defaye, G., Vignais, P. M., and Vignais, P. V. (1974) Partial purification of an atractyloside-binding protein from mitochondria. *FEBS Lett.* 46, 149–153.
- (22) Rey, M., Mrázek, H., Pompach, P., Novak, P., Pelosi, L., Brandolin, G., Forest, E., Havlicek, V., and Man, P. (2010) Effective removal of nonionic detergents in protein mass spectrometry, hydrogen/deuterium exchange, and proteomics. *Anal. Chem.* 82, 5107–5116.
- (23) Zhang, Z., and Marshall, A. G. (1998) A universal algorithm for fast and automated charge state deconvolution of electrospray mass-to-charge ratio spectra. *J. Am. Soc. Mass Spectrom.* 9, 225–233.
- (24) Block, M. R., Pougeois, R., and Vignais, P. V. (1980) Chemical radiolabeling of carboxyatractyloside by [¹⁴C]-acetic anhydride: Binding properties of [¹⁴C]-acetylcarboxyatractyloside to the mitochondrial ADP/ATP carrier. *FEBS Lett.* 117, 335–340.
- (25) Brandolin, G., Doussiere, J., Gulik, A., Gulik-Krzywicki, T., Lauquin, G. J., and Vignais, P. V. (1980) Kinetic, binding and ultrastructural properties of the beef heart adenine nucleotide carrier protein after incorporation into phospholipid vesicles. *Biochim. Biophys. Acta* 592, 592–614.
- (26) Rey, M., Man, P., Brandolin, G., Forest, E., and Pelosi, L. (2009) Recombinant immobilized rhizopuspepsin as a new tool for protein digestion in hydrogen/deuterium exchange mass spectrometry. *Rapid Commun. Mass Spectrom.* 23, 3431–3438.
- (27) Klingenberg, M. (2008) The ADP and ATP transport in mitochondria and its carrier. *Biochim. Biophys. Acta* 1778, 1978–2021.
- (28) Dahout-Gonzalez, C., Nury, H., Trézéguet, V., Lauquin, G. J. M., Pebay-Peyroula, E., and Brandolin, G. (2006) Molecular, functional, and pathological aspects of the mitochondrial ADP/ATP carrier. *Physiology* 21, 242–249.
- (29) Bamber, L., Harding, M., Butler, P. J., and Kunji, E. R. (2006) Yeast mitochondrial ADP/ATP carriers are monomeric in detergents. *Proc. Natl. Acad. Sci. U.S.A.* 103, 16224–16229.
- (30) Bamber, L., Harding, M., Monne, M., Slotboom, D. J., and Kunji, E. R. (2007) The yeast mitochondrial ADP/ATP carrier functions as a monomer in mitochondrial membranes. *Proc. Natl. Acad. Sci. U.S.A.* 104, 10830–10834.
- (31) Bamber, L., Slotboom, D. J., and Kunji, E. R. (2007) Yeast mitochondrial ADP/ATP carriers are monomeric in detergents as demonstrated by differential affinity purification. *J. Mol. Biol.* 371, 388–395.
- (32) Nury, H., Manon, F., Arnou, B., le Maire, M., Pebay-Peyroula, E., and Ebel, C. (2008) Mitochondrial bovine ADP/ATP carrier in detergent is predominantly monomeric but also forms multimeric species. *Biochemistry* 47, 12319–12331.